INTERNATIONAL ATOMIC ENERGY AGENCY
UNITED NATIONS EDUCATIONAL, SCIENTIFIC AND CULTURAL ORGANIZATION
INTERNATIONAL CENTRE FOR THEORETICAL PHYSICS
I.C.T.P., P.O. BOX 586, 34100 TRIESTE, ITALY, CABLE: CENTRATOM TRIESTE

H4.SMR/453-13

TRAINING COLLEGE ON PHYSICS AND CHARACTERIZATION OF LASERS AND OPTICAL FIBRES

(5 February - 2 March 1990)

EXCIMER LASERS: STATUS AND PERSPECTIVES

T. Letardi

ENEA
Centro Ricerche Energia
Roma, Frascati 00044
Italy

ISSN/0393 6333

RT/TIB/89/27

S. BOLLANTI, T. LETARDI

EXCIMER LASERS: STATUS AND PERSPECTIVES

COMITATO NAZIONALE PER LA RICERCA E PER LO SVILUPPO DELL'ENERGIA NUCLEARE E DELLE ENERGIE ALTERNATIVE

ENEA
COMITATO NAZIONALE PER LA RICERCA E PER LO SVILUPPO
DELL'ENERGIA NUCLEARE E DELLE ENERGIE ALTERNATIVE

EXCIMER LASERS: STATUS AND PERSPECTIVES

S. BOLLANTI, T. LETARDI
ENEA - Dipartimento Tecnologie Intersettoriali di Base, Centro Ricerche Energia Frascati

Presented at the NATO-ASI "NON EQUILIBRIUM PROCESSES IN PARTIALLY IONIZED GAS" (Acquafredda di Maratea, 4-17/6/89)

RT/TIB/89/27

Testo pervenuto nel luglio 1989
Progetto ENEA: Tecnologie Ottiche ed Elettroottiche (OP)

EXCIMER LASERS: STATUS AND PERSPECTIVES

S. Bollanti, T. Letardi

ENEA, Dip. TIB, U.S. Fisica Applicata, CRE Frascati,
C.P. 65 - 00044 - Frascati, Rome, Italy

ABSTRACT

In this paper a status of the art on the excimer lasers is reported. After some general remarks, attention is fixed on rare gas halide lasers (RGH), in particular on the self-sustained discharge pumped ones. Problems related to a stable discharge developement are considered and related technological requirements are deduced. Considerations on the propagation of light beams in inverted media show the best way to exploit the active volume. Moreover, a brief review of excimer lasers with unconventional characteristics is done and finally few examples of experimental techniques to measure relevant laser parameters are reported.

1. INTRODUCTION

With the term "Excimer Laser" we intend to refer to lasers which use, as active medium, biatomic molecules which are bound only in the excited electronic states and unbound, or only weakly bound, in the ground state (Excited dimers).

These molecules decay emitting one photon with energy of few eV, that is with wavelength ranging between visible and VUV.

The first experimental evidence of laser emission from excimer system has been done on 1970 by Basov et al.[1] The availability of efficient laser sources emitting in the UV was regarded as an extremely interesting event because it disclosed new experimental possibilities: indeed, UV radiation is absorbed more efficiently by most part of materials, metals and non metals, even by those materials (gold, silver..) which are highly reflecting to the IR radiation.

The lower wavelength reflects in lower diffraction limited divergence angle, i.e. possibility of smaller minimum beam radius, which scales as λ, and higher power density in the focal region, which scale as λ^{-2}.

Moreover, the photon energy is high enough to excite in a single step electronic transitions, i.e. laser sources at this wavelength are very interesting for photochemical reactions.

Later on, the observed photoablative mechanism of materials,[2] strictly connected with the photochemical ability of breaking chemical bonds, opened the possibility of removing organic materials by means of a direct, non thermal process,

reducing the temperature increase in the non ablated material to extremely low values.

The applications in the years following the operation of excimer lasers confirmed these possibilities, and the list can now be completed with the mention of very sophisticated laser systems which are used for efficient x-ray sources, for pumping x-ray lasers and, last but not least, as driver for inertial confinement fusion.

Such a large spectrum of applications has been possible also for the flexibility of this laser source, with respect to peak power, average power, pulse timewidth, etc., as it will be described in the following.

2. DESCRIPTION

A classification of excimer lasers can be done based on the different active media employed. The first excimer lasers developed were the rare gas dimers ones (Xe_2^*[λ = 172 nm], Ar_2^*[λ = 126 nm], Kr_2^*[λ = 146 nm]), all emitting in the ultraviolet spectral region, with the laser transitions taking place between excited Rydberg states and unbound ground states;[1,3] typically they reach energies of the order of 1 J.

Also mercury halides, like HgCl, HgBr and HgI, present excimer characteristics, with laser transitions between an excited bound state and a weakly bound ground state. They emit in the visible region of the spectrum, respectively at λ = 557.6 nm, λ = 501.8 nm and λ = 441.2 nm, and then can be efficient sources for the blue-green light.[4] There are many other classes of excimer lasers and for a detailed description see reference.[5]

Nowadays the most studied and promising excimer sources are the rare gas halides ones (RGH), whose schematic potential energy curves are shown in Fig. 1. The interaction between the rare gas M (ns^2np^6) and the halogen X (ms^2mp^5) in their ground state is of covalent character and gives rise to two molecular states, different from each other for the orientation of the p orbital of X lacking in one electron with respect to the molecular axis. In fact when the X's p orbital without one electron is along the molecular axis, the repulsion is lower than when it is orthogonal and so a rather flat (little bound in the case of XeCl and XeF) ground state $^2\Sigma$ and a repulsive $^2\Pi$ state will result(*).

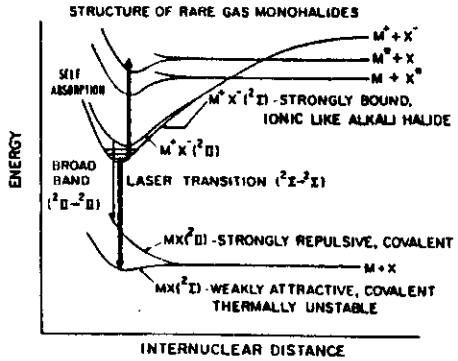

Fig.1. Schematic potential energy diagram illustrating the electronic structure of the rare gas monohalides.

(*) The spin-orbit coupling interaction is not taken into account.

The first two excited states correlate with M^+ and X^- and are strongly bound as a result of the Coulomb interaction between the positive, ionized rare gas and the negative, electron attached halogen. As in the ground state configuration, here also there are a $^2\Sigma$ and a $^2\Pi$ states, with the first one the more bound; the binding energy ranges from 1 eV to several eV, going from the heavier to the lighter species. The main electronic transition goes from the excited state $^2\Sigma$ to the ground state $^2\Sigma$ and, observing the fluorescence spectrum at very low pressure, it is possible to distinguish several lines corresponding to transition from different upper vibrational states to the ground state, lines that disappear at high pressures because of collisional quenching (Fig. 2).[6] In the case of XeCl*, owing to the little bond in

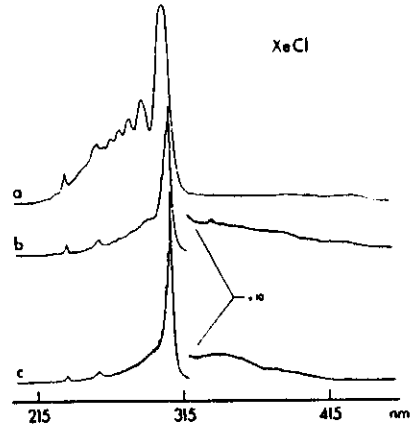

Fig.2. Spontaneous emission spectra of XeCl* at different pressures (without buffer gas): (a) 1.7 Torr; (b) 6 Torr; (c) 26 Torr [6].

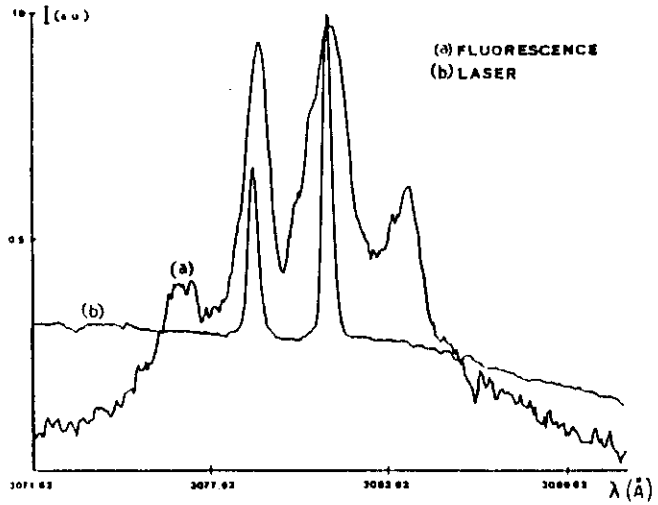

Fig.3. Spontaneous (a) and stimulated (b) emission spectra from a

Table 1. Radiative lifetimes and emission wavelengths on $^2\Sigma.^2\Sigma$ transition of RGH molecules (all the references in [5]).

RGH	τ [ns]	λ [nm]
NeF	2.6	108
ArF	4.2	193
ArCl	--	175
KrF	9.0	248
KrCl	--	222
KrBr	--	206
XeF	16	351
XeCl	11	308
XeBr	17	282
XeI	12	253

the ground state, with a high resolution spectral measurement it is possible to observe transitions from the v = 0 vibrational state in the upper level to four ones of the lower level, as reported in Fig. 3.[7] Here also the laser emission is shown, that, as the fluorescence intensity of the two central lines is comparable, takes place on two different transitions.

In Table 1 radiative lifetimes and emission wavelengths are reported for several RGH molecules.

3. PUMPING SCHEMES FOR RGH LASERS

The pumping process allows the transfer of energy, usually stored in a capacitor bank, to the active medium. To do this, electrostatic energy is transformed in a suitable form of energy which can be coupled efficiently to the gas contained in the cell.

The systems used as pumping processes are: electron beam, proton beam, particles from nuclear reactions, radio frequency, self-sustained electric discharge.

Usually, at each pumping process different characteristics of the laser source correspond, so that one can say that the choice between the different pumping source, at the end, will be dictated by the specific application.

In the electron beam pumping[8,9] an electron beam, generated by a suitable accelerator, enters the gas region through a thin, low Z window. The thickness will depend on the compromise between the requirement of withstanding the gas pressure (some bars) and the requirement of minimizing the electron energy losses in crossing the window. Materials as mylar, aluminum, titanium with thickness between 5 and 50 μm are normally used.

The power density dissipated in the gas by the electron beam $P_{\parallel}$ can be expressed as a function of electron current density J and specific energy loss in the gas dE/dx (eV/cm)

$$P_{\parallel} = J \frac{dE}{dx} \qquad (1)$$

As an example, for 500 keV electrons propagating in Ar at 3 bar is dE/dx = 8 keV/cm, so that for J=1 kA/cm^2 pumping densities up to 8 MW/cm^3 can be achieved.

The lower limit of the electron energy is determined by the losses in the entrance window at a level > 200 keV, while a maximum energy of few MeV is permitted if an efficient coupling of the energy to the gas is required. The main advantages of this technique are the possibility of easily scaling to systems with large volumes (i.e. with large energy/pulse), and the possibility of achieving high pumping density, i.e. high peak power pulses, so that it is generally used in inertial confinement fusion drivers,[10] while their use in small laboratories or as commercial systems is not convenient for complexity, radiation problems, and limited lifetime of some components (input window) which require continuous technical assistance.

In the devices which use radio frequency (RF) power as pumping source the arrangement which has been tried very succesfully[11] consists of an RF source, an impedance matching circuit and two electrodes, between which a small insulator tube containing the gas is put. The gas is preionized, and then the RF pulse is applied to the electrodes producing a diffuse discharge in the gas.

Interesting results have been obtained using glass or ceramic tubes with diameters < 1 mm, and length around 30 cm. The RF frequency is typically around 1 GHz, and the pumping power is about 10 kW/cm^3.

The advantages of this technique are:
- electrodless discharge, so that all the gas eventually could be contained in a long life, sealed chamber
- high repetition rate, up to 100 kHz, because the gas is quickly cooled by means of diffusion to the walls
- long pulses, up to hundreds of nanoseconds.

These characteristics approach a quasi-c.w. working operation.

The disadvantages are:
- low efficiency
- small active volume
- low energy/pulse.

Best results obtained up to now are:
- energy per pulse > 1 μJ
- repetition rate > 10 kHz
- pulse length > 300 ns
- average power > mW.

These performances are interesting for sources used in material processing.

Proton pumping[12,13] is quite similar to e-beam pumping, in that it uses the energy lost by fast particles moving in the gas. It differs from e-beam pumping because, due to the higher dE/dx, it could realize higher pumping power density. Anyway, the technology is more severe: proton beam sources are more difficult than e-beam ones, the entrance window for proton beams must be extremely thin (few microns); few successful results have been reported, with low efficiency and low performances.

Nuclear pumping[14] is another kind of particle beam pumping: it uses the fission fragments as energetic particles. The interest in this technique lies on the fact that high energy density can be stored in a fissionable material: up to ≈ 10^{11}

J/cm^3, it is 10^9 times the energy density in electrostatic capacitors. Some results have been obtained with low efficiency.

In the self-sustained discharge excitation[15] the laser chamber consists of two conveniently shaped electrodes between which is put the gas to be excited. Typically, few torrs of the reacting species (Xe or Kr, with F_2 or HCl) are mixed with some bars of a noble gas (usually Ne); a pulsed ionizing radiation (U.V., X-ray, electrons) creates a suitable electron density, so that when a charged capacitor is connected to the electrodes an electric discharge can develop in the conducting gas. The laser chamber can take different shapes, depending also in the specific preionization source to be used.

In the case of preionization by means of u.v.light the radiation is created by means of sparks (see Fig. 4) near the discharge region.

In the case of X-rays (Fig. 5), the source consists of an external diode in which an electron emitting cathode is put near a high voltage (50 kV-100 kV) anode. The bremsstrahlung produced X-rays enter the laser chamber through a thin, low Z material window (usually, 0.5 mm Al window is a satisfactory solution).

In every case, the pulse of the ionizing radiation must be short enough in time. Indeed, the quality of the discharge depends not on the total number N_e of electrons produced per cm^3, but on the maximum preionization density n_e which is lower then N_e due to electron attaching species in the gas, which limit the lifetime of free electrons. Indeed, if we indicate with $n_e(t)$ the electron density at time t, with τ the lifetime of free electrons, with R the production rate of electrons, constant in a time interval T, we can easely see that the preionization density at the end of the pulse T is

$$n_e(T) = \tau R\left[1 - e^{(-T/\tau)}\right] \tag{2}$$

and the total number of electrons produced (per cm^3) is

$$N_e = RT \tag{3}$$

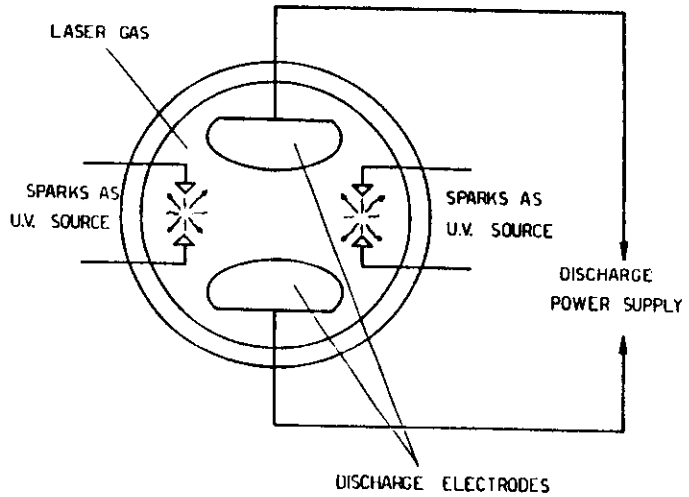

Fig.4. Laser pumped by self-sustained discharge with

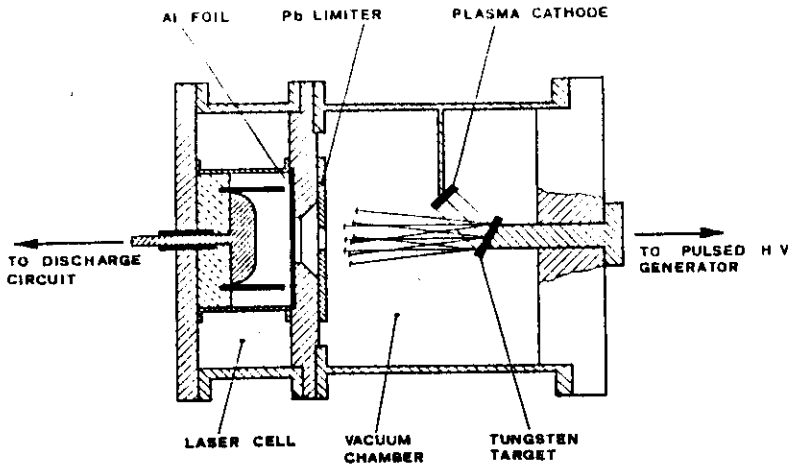

Fig.5. Laser pumped by self-sustained discharge with x-ray preionization.

so that the ratio between maximum number density $n_e(T)$ and the total number of produced electrons N_e is

$$\frac{n_e(T)}{N_e} = \frac{\tau}{T}\left[1 - e^{(-T/\tau)}\right] \tag{4}$$

Only if $T \ll \tau$ is $n_e(T) \approx N_e$.

Being $\tau \approx 100$ ns, at the normally used concentration of HCl or F_2, this would be the order of magnitude of the pulsewidth of the preionization pulse.

From the electrical point of view, the circuit can be represented as in Fig. 6 a) and b).

In both cases, only most relevant parameters for the discharge are reported. A capacitor (C or C1) is charged at a high voltage V_0, and then connected to the laser head directly by means of a switch S (case a) or after the transfer of energy to a second capacitor bank (case b).

In every case, the final system consists of an RLC discharge circuit, in which we have indicated only the main parameters: the resistance of the discharge R_i (omitting all the parasitic resistances), the total inductance of the discharge circuit L, and the energy storage capacitor C.

The normal operating characteristics impose severe constraints on the maximum permitted values of the parasitic inductance L. Indeed, the discharge resistance usually ranges between 0.1 Ω and 1 Ω, while capacitors of many tens of nanofarad (up to hundreds of nanofarad) must be used to store the energy at the voltage suitable for the discharge. In these conditions, usually an oscillating discharge develops, because practically always it is

$$\frac{4}{R^2}\frac{L}{C} \gtrsim 1 \tag{5}$$

Moreover, the period T of the oscillating discharge current, given by

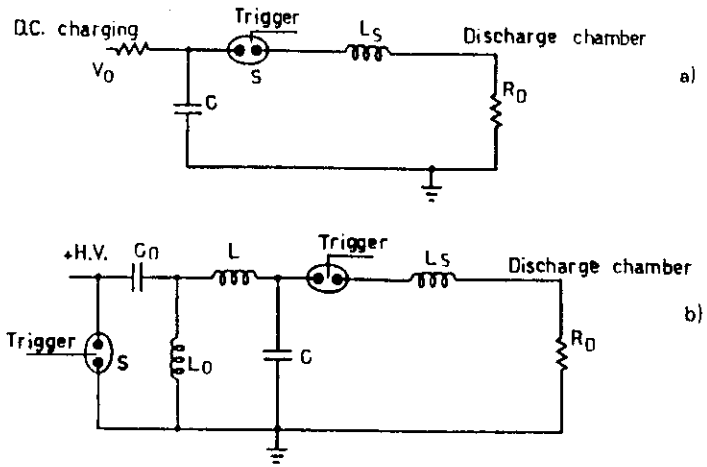

Fig.6. Schematic diagram of the discharge pumping circuit: (a) D.C. charging circuit; (b) resonantly charging circuit.

$$\frac{1}{T} = \frac{1}{2\pi} \sqrt{\frac{1}{LC} - \frac{R^2}{4L^2}} \tag{6}$$

defines the useful pumping period and must be as short as possible because the discharge is stable only for times shorter than a microsecond. This condition can be expressed by means of the fraction of energy delivered to the gas in the first half period T/2, that is (see Flora, ENEA Internal Report)

$$\delta_d = 1 - e^{-T/\tau} \tag{7}$$

where $\tau = 2L/R$ so that L must satisfy the condition

$$R \gg \sqrt{\frac{L}{C}} \tag{8}$$

if efficient utilization of the stored energy is required.

Typical behaviours of the discharge current and voltage are shown in Fig. 7.

As it has been previously mentioned, only uniform (diffuse) discharges are useful for laser action. When the discharge collapses in arcs the laser emission terminates.

On short time scale, a bad development of the discharge can be related with an inadequate level of preionization, that is initial electron number density, also in connection with the risetime of the subsequent discharge voltage, if it is applied after the end of the preionization. For each working condition there is a minimum preionization electron density required, whose estimation can be done following this

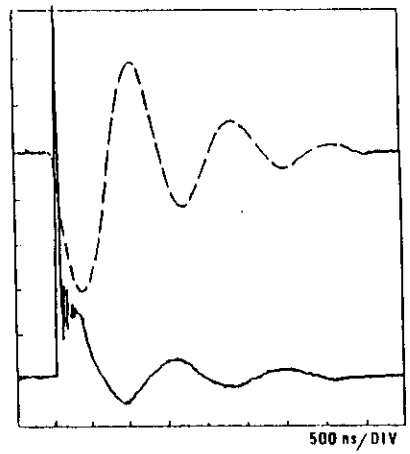

Fig.7. Time resolved discharge voltage (solid line) and current (dashed line). 8.8 kV/div for voltage, 40 kA/div for current.

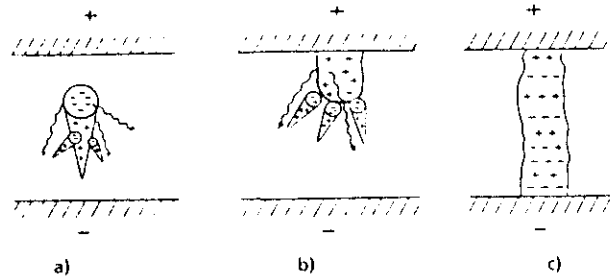

Fig.8. Schematic diagrams showing (a) streamer development around a single primary electron avalanche after its space-charge field has grown beyond a certain critical value; (b) continuous backward propagation of the cathode-directed plasma streamer after the arrival of the primary avalanche head at the anode; (c) complete bridging of the electrode gap by the plasma streamer [16].

electric field develops an electron avalanche, whose negative head is growing more and more, leaving behind itself positive ions. Consequently, also the corresponding space charge field will be stronger and stronger, until it will become comparable with the applied electric field, finally causing the formation of a streamer through the discharge gap, as shown in Fig. 8. On the other hand, all these avalanches can give a glow discharge only when their heads will superimpose each other, in such a way to uniform the charge distribution and to reduce the gradients of the space charge field. A condition to be met after these preliminary remarks is that when the space charge field becomes comparable with the external field, the avalanche heads must be superimposed each other. This sets an upper limit to the initial

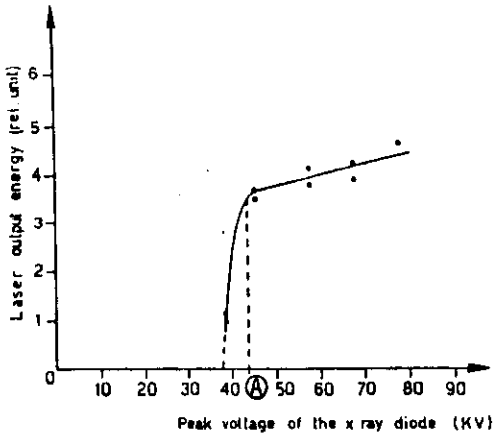

Fig.9. Laser output energy vs preionization intensity. XeCl* laser mixture pressure: 3 atm; discharge capacitance: 0.48 μF; charging voltage: 50 kV.

In addition to this requirement, if the high voltage is applied to the laser cell after the end of the preionization pulse, the drift of the electrons away from the cathode in the pre-breakdown phase has to be taken into account. For a good discharge the voltage risetime must be short enough to not allow to the electron depleted region near the cathode to become larger (in the electric field direction) than the electron avalanche head at the critical point (i.e. space charge field = external field). This requirement adds to the previous one, giving voltage risetimes of the order of tens of nanoseconds and preionization electron number densities of $\approx 10^5 \div 10^6$ cm^{-3}.[17]

If we plot the laser output energy vs the preionization density in a practical device we get a result as depicted in Fig. 9. It is clear that above point A the laser output depends very weakly on the preionization density, and a useful working point can be set at a value of 3-4 times the preionization density of upper knee.

4. CHARACTERISTICS OF THE ACTIVE MEDIUM

The mechanisms through which the RGH excited molecules and the laser radiation are formed and extinguished during a discharge are very complex. Big kinetic codes have been developed with the aim of reproducing the laser working characteristics, taking into account many kinds of reactions, the electron energy distribution function and the coupling of the discharge region with the external circuit,[18] following the general scheme reported in Fig. 10.

Related to the big effort around kinetic codes there is the spur of understanding the processes which generate instabilities in the discharge on long timescale, its collapse in arcs and premature termination of the laser action due to the reduction of the discharge volume.[19] One possible explanation of this fact deals with local depletion of the halogen donor: suppose that there are little disomogeneities in the electron spatial distribution; where the electron density is higher, due to the attachment process the number of halogen molecules will decrease; in turn, in this region the electron losses by attachment will be lower and the electrons will grow at an higher rate than in the other regions of the discharge. This "positive feedback" can cause the developments of arcs which destroy the glow discharge and, due to their very low resistance, do not absorb more energy from the

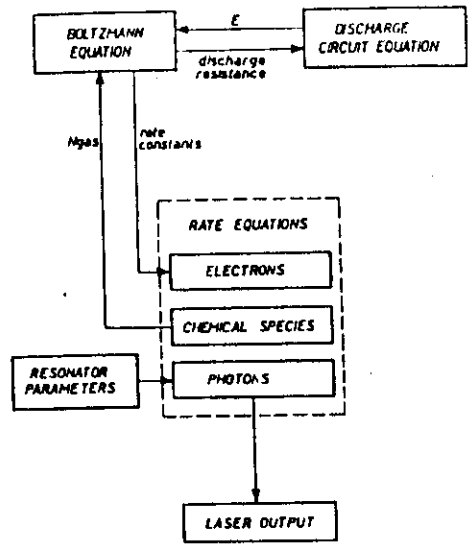

Fig.10. General scheme of a simulation code for discharge pumped RGH lasers. E = electric field.

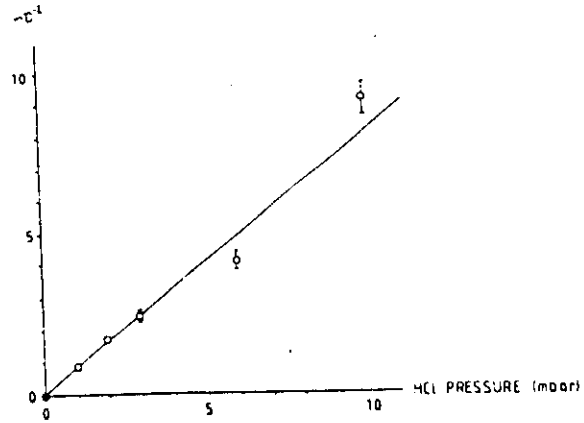

Fig.11. A plot of τ^{-2} against HCl partial pressure, for 1 bar Ne, 20 mbar Xe mixture [20].

external circuit, producing no more photons. The duration τ of the glow, useful discharge has been put in relation with the initial density of the halogen donor in the case of the XeCl* laser with HCl,[20] as reported in Fig. 11.

The shape of the electrodes, which must create an electric field as uniform as possible in the discharge region, affects the time length of the diffuse discharge: ideally the electric field would be constant in the discharge region and it would go

to zero outside, in order to avoid flow of current outside the useful region. Many solutions have been investigated[21,22] which reasonably approximate the required conditions.

In discharge pumped lasers the pumping density is a very important and critical parameter. It is obvious that, increasing the power delivered to the gas, it is possible to reach higher output energies, but on the other hand this can also increase the rate at which instabilities develop in the discharge.[19b] Moreover, going at higher energies stored in the main discharge bank usually leads to a decrease of the discharge efficiency, because (seen from a macroscopic point of view) the discharge resistance drops and so also the power dissipated on it.

Related to the power density deposited into the gas is an important parameter, the small signal gain coefficient g_0. From the theory we know that:

$$g_0 = \sigma n_0 \tag{9}$$

where:
σ = stimulated emission cross section
n_0 = initial population inversion.

Depending on the kinetic processes during discharge, the number density of the active molecules formed is roughly proportional to the deposited power density and so g_0 is, from (9):

$$n_0 = \frac{\eta_f P_d \tau}{h\nu} \tag{10}$$

where:
- η_f = formation efficiency = energy in active molecules/deposited energy
- τ = active molecules lifetime
- P_d = deposited power density.

For typical values in the case of XeCl* laser ($\sigma = 4.5\times10^{-16}$ cm^2, $\tau \approx 2$ ns, $h\nu \approx$ 4 eV, $\eta_f \approx 0.2$):

$$g_0[\mathrm{cm}^{-1}] \approx 0.3\, P_d[\mathrm{MW/cm^3}] \tag{11}$$

It is evident that to obtain a gain coefficient of the order of 10%/cm a very high power density, in the range of MW/cm^3, is required.

Usually, when operating with electric discharges, common values of P_d are between 0.1 to 0.5 MW/cm^3, giving a gain coefficient up to 10%/cm, which mantains a linear dependence on P_d, as shown in Fig.12a, where experimental data for XeCl* laser are reported; the angular coefficient is ≈ 0.33, very similar to the estimated one.[23]

With the electron-beam pumping technique higher power density deposition can be achieved, up to several MW/cm^3, but in this case the behaviour of g_0 vs. P_d is no more linear. This can be explained with: 1) the smaller formation efficiency and 2) the shorter lifetime of the active molecules. In fact with e-beam pumping there is need of a high mean electron energy in order to obtain a uniform excitation of the gas and this can favour some formation channels (e.g. through direct ionization) that are not necessarily the most efficient. Instead with a discharge pumping the electrons are continuously accelerated, from almost zero energy, from the applied electric field, leading to the activation of different channels for the excimer formation so that finally the lost energy is lower. For the same reason, in the case

a)

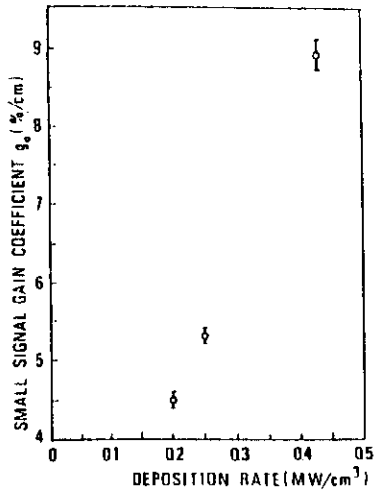

b)

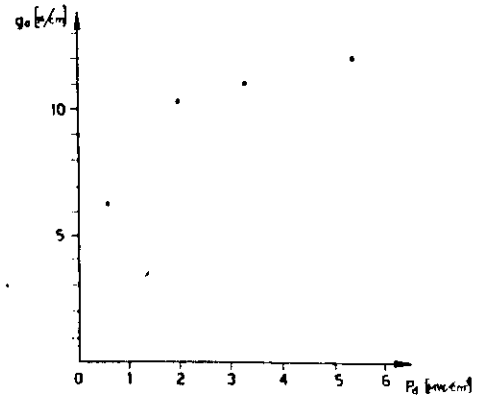

Fig.12. Small signal gain coefficient g_0 vs energy deposition rate in (a) a discharge pumped [23] and (b) an e-beam pumped [8] XeCl active medium.

of e-beam the quenching rate of the active molecules is faster and this results in a shorter lifetime.

An experimental result which shows a saturate behaviour of g_0 vs. P_d is reported in Fig.12b.[8]

5. OSCILLATOR, AMPLIFIER AND EXTRACTION EFFICIENCY

It is possible to understand the importance of g_0, together with other two parameters, α, non saturable absorption coefficient, and I_s, saturation intensity, examining the equation which controls the propagation of a collimated beam, with initial intensity I_0 and pulse duration much longer than the upper state lifetime, in an inverted medium with homogeneous line broadening, say in x direction:

$$\frac{dI(x)}{dx} = \left| \frac{g_0}{1 + I(x)/I_s} - \alpha \right| I(x) \qquad (12)$$

From the equation it is clear that the gain term decreases with increasing intensity and reaches one half of the initial value when the beam intensity is equal to the saturation intensity. At the same time the losses don't change, leading to a constant reduction of the amplification, until, in an infinitely long active medium, the intensity reaches its asymptotic value, that can be obtained equating to zero dI/dx:

$$I(+\infty) = I_{max} = I_s \left(\frac{g_0}{\alpha} - 1 \right) \qquad (13)$$

The amplification of light beams inside laser oscillators has been extensively studied[24] to try to optimize the output intensity or the extraction efficiency (defined as the ratio between output energy and energy stored in the active molecule) changing the oscillator length, L, or the output mirror reflectivity, R. In Fig. 13 a plot of the maximum extraction efficiency vs optimum output coupler is reported for different combinations of $g_0L - \alpha L$.[24b]

These considerations all refer to the case of a flat-flat cavity with a totally reflecting mirror and an output coupler. Indeed this is the configuration that allows to extract the highest energy from the active medium, because involves it completely, but it gives also a poor beam quality, doing no transverse mode

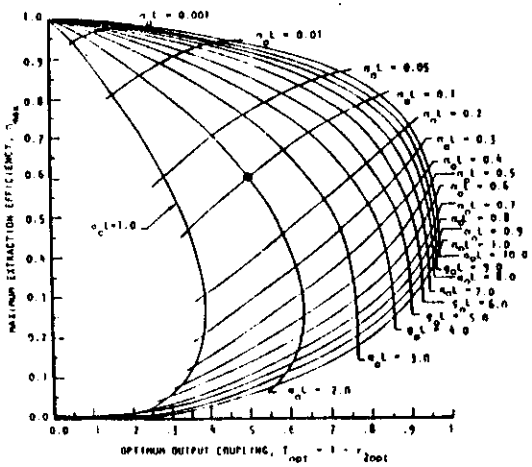

selection and so resulting in high divergent beam, typically with divergence value around some milliradiants.

So, often low energy, high quality beams generated with special cavities are sent in excimers' active media for amplification. Also for an amplifier an extraction efficiency is defined:

a)

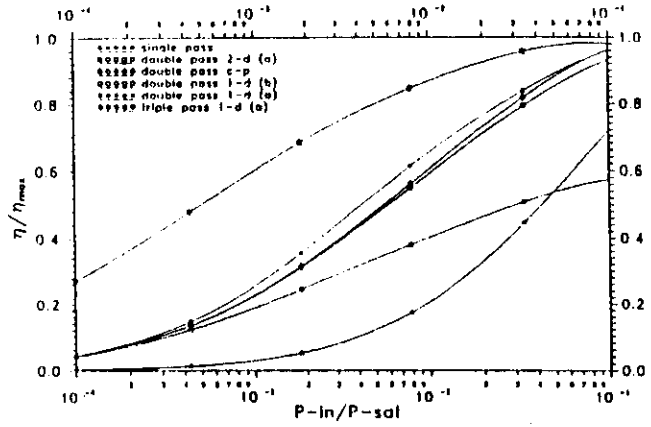

b)

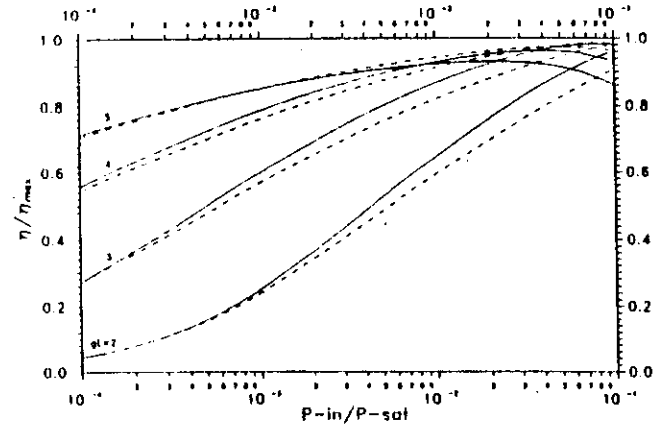

Fig.14. Ratio extraction efficiency/maximum extraction efficiency vs. normalized input power, for: (a) different amplifier configurations (c-p = counter propagating, 1/2-d = expansion in 1/2 dimensions, (a): $h_0/D = 0.05$, (b): $h_0/D = 0.5$, h_0 = input beam diameter, D = amplifier diameter), with $g_0L = 3$, $g_0/\alpha = 10$; (b) different g_0L

$$\eta_{ext}^{am} = \frac{P_{out} - P_{in}}{P_s} \qquad (14)$$

where:
- P_{in} = power at the input of the amplifier
- P_{out} = power at the output of the amplifier
- P_s = saturation power = $(h\nu n_0 V/t) = I_s g_0 V$, maximum extractable power
- V = amplifier active volume.

How to maximize the output power, given the input, that is η_{ext}^{am}, exploiting as better as possible the amplifier active medium? Two basic possibilities are: 1) single passage with collimated beam with diameter equal to the amplifier one; 2) single passage with an expanding beam with output diameter equal to the amplifier one. To understand which one of these two configurations can give the best results, it is better to rewrite the propagation equation (12) for the beam power:

$$\frac{dP(x)}{dx} = g_0\left(\frac{1}{1 + I(x)/I_s} - \frac{a}{g_0}\right)P(x) \qquad (15)$$

For a fixed input power, the increase dP/dx will be higher if the intensity is as low as possible: it is more convenient to work with a collimated beam investing all the active medium. In Fig. 14 calculated extraction efficiencies are reported as function of P_{in}/P_s for different amplifier configurations and g_0L values. For a more exhaustive treatment, we refer you to Ref. 25.

6. MAIN CHARACTERISTICS OF COMMERCIAL EXCIMER LASER SOURCES

In Table 2 some characteristics of commercial systems are reported.

Table 2. Main characteristics of commercial RGH excimer systems

	ArF	KrF	XeCl	XeF
Wavelength [nm]	193	248	308	351
Average power [W]	50	100	150	30
Pulse width [ns]	5-25	2-50	1-300	1-30
Energy/p [J]	.5	2	2	.5
Repetition rate [Hz]	1-1000	1-500	1-500	1-500
Efficiency [%]	1	2	2.5	2
Beam cross section [mm^2]	2 x 4 - 25 x 30			
Beam divergence [mrad]	2 - 6 (< 2)			

7. LASER SOURCES WITH UNCONVENTIONAL CHARACTERISTICS

In some cases, depending on the specific applications, characteristics of the laser beam much different from those available in commercial systems could be required; very advanced systems have been designed in order to have:
- low beam divergence, up to the diffraction limited angle (~ .1 mrad)
- ultrashort pulse, up to the region of femtoseconds

- high energy/pulse, up to the region of many kJ/pulse
- high average power, up to the region of many kW.

A quantity which can express the spectral and spatial quality of a laser radiation is the spectral brightness, that is defined as the energy radiated per unit time, frequency interval, surface and solid angle at a given wavelength. Several methods have been developed to obtain a beam with a good brightness from one or more of the possible improvements.

Low Divergence Beams

The solid angle and surface of emission can be reduced selecting only one or few low transverse modes. This can be accomplished by means of unstable cavities and/or spatial filters.[26] Near diffraction limited beams have been obtained using a SFUR[27] (Self Filtering Unstable Resonator), a confocal, negative branch unstable resonator, with a spatial filter with given aperture in the focus common to the two cavity mirrors, whose schematic diagram is shown in Fig. 15a.[27b] The extraction efficiency in the involved volume is very high, but the mode volume is very small and so the final output energy is reduced with respect to a flat-flat cavity. Another kind of unstable cavity which gives good results on the transverse mode selection is the PBUR (Positive Branch Unstable Resonator)[28], a scheme of which is reported in Fig.15b.

Narrow Bandwidth Beams

Near or single longitudinal mode lasers have been realized by means of intracavity gratings, prisms and etalons. 29 An arrangement of a laser cavity with a line-narrowing element is shown in Fig. 16, together with its effect on the linewidth after several roundtrips. It is evident that the more round trips in the cavity, the more effective the line narrowing becomes.

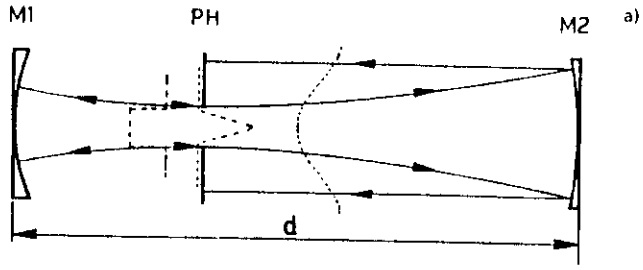

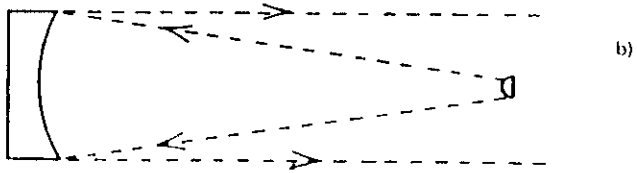

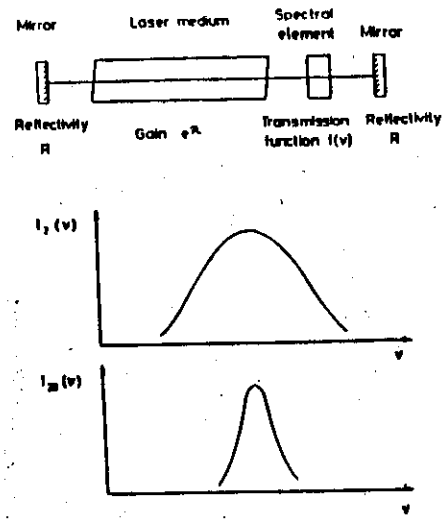

Fig.16. Laser cavity with a line-narrowing element (a) and its effect on linewidth after (b) 2 and (c) 20 roundtrips.

Ultrashort Pulses

To reduce the pulse duration of excimer lasers conventional methods like active and passive modelocking have been employed, obtaining pulses of ≈ 2 ns duration.[30] The use of an intracavity fast Pockels cell allowed to reach laser pulses of ≈ 300 ps;[31] but, to go in the region of pico- or femtoseconds u.v. pulses, at least a double device system is needed, the first device generating the ultrashort pulse, usually with very low energy, in the visible or u.v. region, the second one, the excimer active medium, (after an eventual frequency duplication) acting as amplifier. Usually a CPM (Colliding Pulses Modelocked) dye laser is used as oscillator to generate ultrashort pulses in the visible region; then they are amplified in another dye and frequency doubled before entering the last stage, the excimer amplifying medium. The time width of the amplified pulse has a lower limit set by the limited spectral bandwidth of the excimer media. Anyway, 160 fs pulses have been obtained from a "CPM-dye amplifier-KDP-XeCl* amplifier" chain with 12 mJ final energy;[32a] 80 fs pulses resulted from two KrF* final amplifiers (with a little different initial configuration), which have a gain bandwidth broader than XeCl*, with a final energy of 15 mJ.[32b] More recently 1 TW pulses have been obtained from a XeCl* laser, with a longer pulse, 310 fs, but an higher energy, 300 mJ.[32c]

The most difficult problems to be solved concerning the amplification in excimer media are: the overmentioned temporal lengthening due to the relatively narrow gain bandwidth; the presence of ASE (Amplified Spontaneous Emission), that becomes considerable when the value of g_0L is high (> 1) and can be contained to few percent of the total extracted energy by means of spatial filters;[32] the group velocity dispersion, which causes pulse broadening, because the different spectral components of the pulse propagate with different speeds, and can be compensated introducing systems with negative dispersion;[33] the gain saturation, which is a not completely well understood phenomenon on the femtosecond scale, but surely for

such short pulses the maximum extractable energy is limited by the saturation energy of the active medium:

$$E_{ext} = h\nu\, n\, V = E_s g_0 V \qquad (16)$$

where:

$$E_s = \frac{h\nu}{\sigma}, \text{ saturation energy}$$

In the case of RGH lasers E_s is in the range of 1 mJ/cm^2, so that with a $g_0 \approx 0.1$ cm^{-1} and an active volume of 1l the maximum extractable energy ($\eta_{ext}^{am} = 1$) is ≈ 100 mJ.

Long Pulses

In conventional systems the time length of laser pulses, when the source is operated in the self sustained discharge mode, is shorter than ≈ 200 ns. This is due to the discharge instabilities, which do collapse the diffuse discharge into arcs after few hundreds of nanoseconds, terminating the laser action. On the other hand, some applications would require longer pulses:

- in material processing, when high peak power, with consequent ablative processes, must be avoided;
- when the beam must be transported in fibers (especially for medical applications) because the damage limit of the fibers is associated with peak power, not with average power.

Clearly, these types of applications do not justify the use of e-beam pumping technique which can deliver much longer pulses.

Some techniques have been successfully developed in order to increase the stability of the discharge, and so the timelength of the pulse.

The instability of the discharge can be associated with a halogen donor depletion. Webb et al.[20] succeded in stabilizing the discharge inserting in the circuit external ballast resistors. In this way, microsecond pulse duration, at low efficiency and low energy/pulse, have been achieved.

Quite recently[34] the double pulse technique has permitted the achievement of very long pulses at very high efficiency. The double pulse technique was introduced for the first time by Long et al.[35] To explain the system, we observe that we can distinguish in the process of the self-sustained discharge, two temporal phases: in the first phase (few nanoseconds) we observe in the gas a strong increase of the electron density, which passes from the initial density of about 10^7-10^8 e/cm^3 to the final density of about 10^{14}-10^{16} e/cm^3. In the second phase, the electron density is essentially stationary, and the flowing current pumps the active medium. The two phases are essentially driven by the applied electric field and its optimized value is different for the two phases. Usually, the charged capacitors, with associated output impedance which is in series with the time varying impedance of the discharge, play the double role of electron density multiplication (high electric field) and pumping discharge (low electric field). The use of the same circuit for the two functions does not permit an optimization of the process. Separation of the two functions in two different circuits (prepulse technique or double pulse technique) permitted an increase of efficiency and stability. The same technique, associated with magnetic switches and pulse forming line, has permitted the operation [34] of a system with pulses .5 μs, .5 J/p, efficiency of 2%.

High Energy Pulses

Scaling of excimer laser systems to very high energy per pulse in self-sustained discharge operation has been done for XeCl resulting in a source delivering 60 J/p, in a 120 nsec pulse.[36]

Much higher energy can be obtained in e-beam pumped systems. A KrF fusion device (AURORA) developed at Los Alamos will deliver in the future 10 kJ/p, in a pulse 5 ns long. Presently, 2.5 kJ have been achieved.[37]

High Average Power

Excimer laser sources having average power in the kW range are interesting for material processing (cutting, surface treatments) and for photochemistry applications on industrial scale.

Only combinations on a limited range of energy/pulse and repetition rate are realistic; systems up to now operated or under study consider energy/pulse ranging from a fraction of Joule/pulse to about 10 J/p, with repetition rate ranging from few kHz to 100 Hz. In every case, very severe problems have to be solved: for gas flow, which must have a speed in the discharge region of about 100 m/s; for switches, which would be of the saturable magnetic type, and for damping of shock waves, which modulate the gas density and reduce the quality of the laser beam. Average powers near 500 W for XeCl and KrF systems have been recently achieved.[38]

8. EXPERIMENTAL MEASUREMENTS

From a more experimental point of view, it is interesting to see how some macroscopic parameters that have been introduced before can be measured.

Gain, absorption and saturation intensity measurements

If a light beam enters in an active medium with intensity much lower than the medium saturation intensity, Eq. (12) can be rewritten as follows:

$$\frac{dI(x)}{dx} = (g_0 - \alpha) I(x) \qquad (17)$$

This equation can be easily integrated to give:

$$I(x) = I_{in} e^{(g_0 - \alpha)x} \qquad (18)$$

This behaviour is true if $I(x) \ll I_s$, so if at the output of the active medium (say, $x = L$) this condition still holds, the intensity will be grown exponentially all the way long and:

$$\frac{I_{out}}{I_{in}} = e^{(g_0 - \alpha)L} \qquad (19)$$

With this simple formula it is possible to mount a setup for the measure of the "net" gain, i.e. $g_0-\alpha$, injecting a probe beam at the laser wavelength in the excited active medium and carefully controlling the input and output intensities; nevertheless there are still other few considerations to be done.

The first is that it is desirable to distinguish the two parameters, g_0 and α, because also their ratio is important to characterize a laser (see Eqs. (13) (15)); the second is about the spectral and temporal dependance of g_0 and α. As far as the spectral dependance is concerned, it can help to discriminate the two parameters. In fact $g_0(\lambda)$ receives contribution only from the excimer and is sensitively different from zero only around the wavelengths correspondent to the main RGH transitions, following the behaviour of the fluorescence in Fig.3; on the contrary $\alpha(\lambda)$ sums all the contributions of the species which form during the discharge in the active volume and, in the case of $XeCl^*$ from a mixture Ne/Xe/HCl, it has been shown that the stronger absorbers (Xe^+, Cl^-, Ne^{**}) have almost the same absorption at λ_L = 308 nm (laser wavelength) and at longer λ (λ > 311 nm), where the gain is negligible. In this way it is possible to estimate the value of $\alpha(\lambda_L)$ measuring the absorption coefficient out of the gain spectral region and estrapolating it at the laser wavelength, and then measure the net gain at λ_L, finally deducing $g_0(\lambda_L)$.

As regards the temporal dependance of g_0 and α, due to the pulsed operation of excimer lasers, it is convenient to use a long pulse probe laser, in such a way to follow directly, from the time behaviour of the output probe pulse with respect to the input one, the time behaviour of the gain or absorption.

An experimental setup for small signal gain and absorption coefficient measurements is schematically shown in Fig. 17. The probe beam comes from a dye laser, a visible, tunable source, is frequency doubled and sent into the active medium, being examined both in input and at the output. If the value of the saturation intensity of the excimer medium is not known, it is possible to check that the requirement on the intensity ($I(x) \ll I_s$, $0 < x < L$) is satisfied by simply trying to see if Eq. (19) is true for different values of I_{in}. Results for temporal and spectrally resolved g_0 and α are reported in Figs. 18-19.[23]

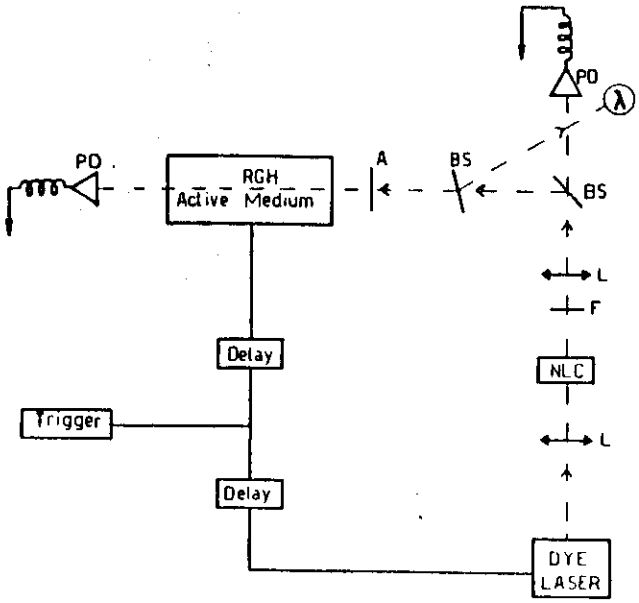

Fig.17. Experimental scheme for g_0 and α measurements. L = lens; NLC = non linear crystal; F = u.v. filter; BS = beam splitter; A = attenuator; PD = photodiode.

a)

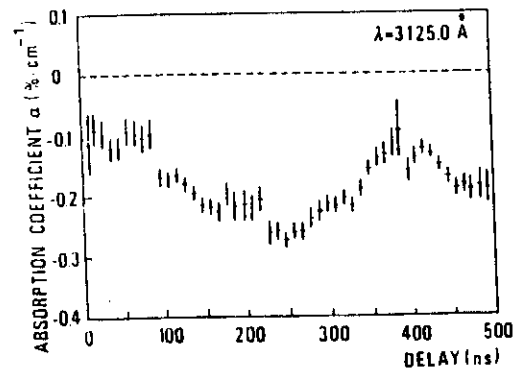

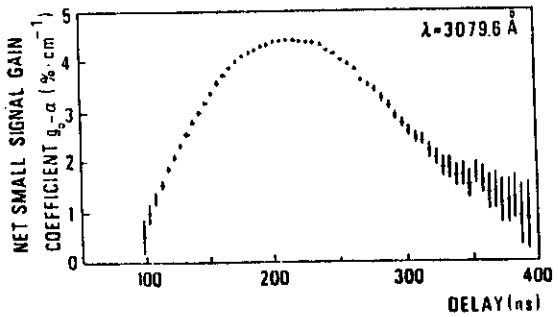

b)

Fig.18. (a) Absorption coefficient α vs time for λ = 3125 Å; (b) net small signal gain coefficient g_0-α vs time for λ = 3079.6 Å. T = 0 corresponds to the beginning of the discharge voltage risetime. Both measurements have been done with a pumping power density of 200 kW/cm [23].

The measure of the saturation intensity I_s is little more difficult and usually estimates of this parameter are given with large errors.[8,39] A more exact evaluation of I_s can be accomplished by using Eq. (12) in a different way. Suppose to send a laser probe beam into an laser oscillating with the same laser wavelength and with the probe beam intensity, I_p, much lower than the intracavity intensity, I_c. The Eq. (12) for I_p propagating in the laser medium is:

$$\frac{dI_p(x)}{dx} = (g-\alpha)I_p \qquad (20)$$

where

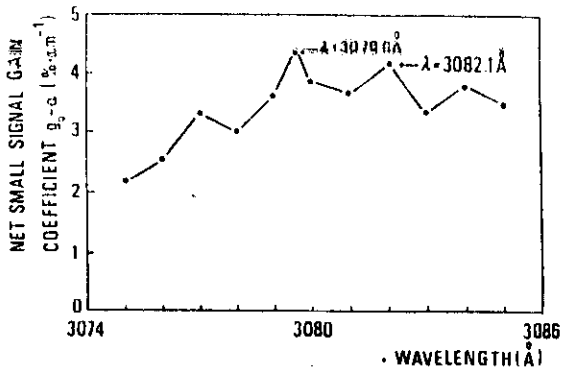

Fig.19. Net small signal gain coefficient g_0-α vs wavelength λ, for delay time of 230 ns and a pumping power density of 200 kW/cm³ [23].

$$g = \frac{g_0}{1+(I_c+I_p)/I_s}$$

As $I_p \ll I_c$ for $0 < x < L$ (L = active medium length), this equation simplifies:

$$\frac{dI_p(x)}{dx} = \left(\frac{g_0}{1+I_c/I_s} - \alpha\right) I_p \qquad (21)$$

If the time width of the probe pulse is rather shorter than the laser oscillation, it is reasonable to think that during its propagation the probe pulse meets a rather constant intracavity intensity, so that the coefficient in front of I_p in (21) is constant and the growth of I_p is exponential.

Measuring I_p^{out}/I_p^{in}, that is $(g_0/(1+I_c/I_s) - \alpha)$, and knowing I_c, g_0 and α, it is possible to deduce the value of I_s. Several points can be taken, varying I_c, and then g (not g_0), by changing the output coupler reflectivity, to reduce the error on the measure.

From a practical point of view, there is the need to distinguish the probe beam at the output of the oscillator from the laser radiation, seen that $I_p \ll I_c$. This can be accomplished by means of windows sealing the active medium at the Brewster angle, so that the oscillator radiation is p-polarized and a s-polarized probe can be extracted nearly without noise. An experimental setup for this kind of measure is reported in Fig. 20. The relative error on this measure can be ≈ 20-25%, while with standard methods it is as high as 50%.

Electron Density Measurements by Holographic Techniques

This technique[40] permits the measurement of electron density in a plasma during the discharge with a sensitivity of the order of $N_e L \approx 10^{16}/cm^{-2}$, if N_e is the electron number density in cm^{-3} and L is the total optical path in the plasma in cm, with time resolution of the order of some nanoseconds. The principle of the method is the following: the refractivity n of a plasma can be expressed as

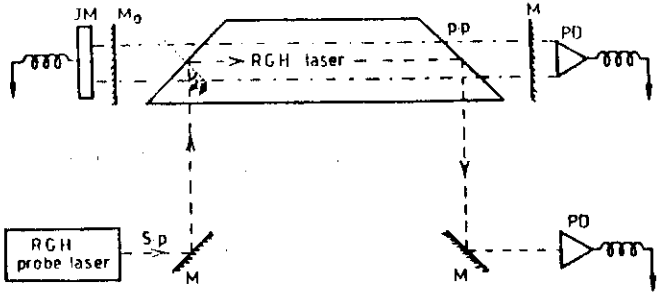

Fig.20. Schematic diagram for an experimental setup for saturation intensity measurement. M = mirror; M_o = output mirror; JM = joulemeter; PD = photodiode.

$$(n-1) = (n_e-1) + \Sigma_k (n_k-1) \tag{22}$$

where (n_e-1) and (n_k-1) are the components due to the electron density N_e and to the heavy particle density N_k. If the radiation frequency is much higher than the plasma frequency and far enough from the resonance frequencies of the heavy particles, Eq. (22) may be approximated by

$$(n-1) = \Sigma_k \left(A_k + \frac{1}{\lambda^2} B_k\right) N_k - 4.47\times10^{-14} N_e \lambda^2 \tag{23}$$

where A_k and B_k are characteristic coefficients of the species considered and λ is the radiation wavelength.

In interferometric measurements of the refractivity of a homogeneous plasma layer of thickness L the normalized fringe shift S caused by introducing an optical path difference is related to the refractivity variation $\Delta(n-1)$ by the expression

$$S = \frac{L}{\lambda} \Delta(n-1) \tag{24}$$

Usually, (n-1) refers to the initial state characterized by $N_e = 0$. From Eqs. (23) and (24) and taking into account that in the visible spectral region the contribution of the heavy particles to the fringe shift is negligible, compared to the electronic contribution, we may write the following expression:

$$S = -4.47\times10^{-14} N_e \lambda L \tag{25}$$

for the normalized fringe shift S of radiation with wavelength λ after an optical path L in a plasma which had a variation N_e in electron number density.

The sensitivity limit of the electron density measurement can be evaluated assuming for the smallest detectable fringe shift the realistic value $S = 0.1$, so that it must be

$$(N_e L) > 1.2\times10^{16}\ \mathrm{cm}^{-2} \tag{26}$$

at the wavelength of ruby laser ($\lambda = 694$ nm).

Preionization Density Measurements by Collecting Electric Charge

Preionization by X-ray or UV radiation provides an effective method for initiating homogeneous discharges in rare gas halide excimers at high pressure. The measurement of the preionization electron number density is required not only in the computation of the characteristics of discharge lasers, but also in the identification of the preionization electrons formation or loss mechanism. The measurements are often made by determining the gas mixture conductivity or electron drift current between two collecting electrodes subject to a given voltage. However, due to a very strong electro-magnetic interference (typically, in the first few μs) arising from the firing of the preionizer, it is difficult to use the laser discharge electrodes as collecting plates. In order to overcome this problem, the preionization electron density has been measured by collecting the electric charge of the drifting electrons. In this way the measurements can be done with a high signal-to-noise ratio. The measurements require rather long (> μs) collecting time, so that they must be done without the electron attaching species in the gas mixture.

An important process which must be taken into account is the ion space charge which develops near the cathode due to the drifting electrons. This space charge field or potential drop can strongly influence the drifting process of the electrons.

A model[41] has been developed to describe the collection of the drifting electrons in presence of space charge.

The main results are: if the ionized region is limited by parallel electrodes of area S, at a distance d, and if n_e is the uniform electron density produced by the preionization, the applied voltage V_0 in order to collect all the electric charge must be

$$V_0 \geq e n_e \frac{d^2}{2\varepsilon_0} = V_{min} \tag{27}$$

If $V_0 < V_{min}$, then the collected electron charge Q will be expressed by

$$Q = S\sqrt{2\varepsilon_0 V_0 n_e e} \tag{28}$$

while when $V_0 > V_{min}$, it will be

$$Q = S d n_e e \tag{29}$$

which is independent of collecting voltage.

REFERENCES

1. N.G.Basov et al., Sov.J.Quantum Electron. 1 (1971), 18.
2. R.Srinivasan and V.Mayne-Bantom, Appl.Phys.Lett. 41 (1982), 576.
3. H.A.Koehler et al., Appl.Phys.Lett. 21 (1972), 198;
   P.W.Hoff et al., Opt.Comm. 8 (1973), 128;
   G.B.Gerardo, A.W.Johnson, IEEE J.Quantum Electron. QE-19 (1973), 748;
   W.H.Hughes et al., Appl.Phys.Lett. 24 (1974), 488;
   W.H.Hughes et al., Appl.Phys.Lett. 25 (1974), 85.
4. J.H.Parks, Appl.Phys.Lett. 31 (1977), 192;
   J.H.Parks, Appl.Phys.Lett. 31 (1977), 297; W.T.Whitney, Appl.Phys.Lett. 32 (1978), 239;
   K.Y.Tang et al., Appl.Phys.Lett. 32 (1978), 226.
5. C.K.Rhodes: "Excimer Lasers", II ed., Springer-Verlag, 1984.
6. J.E.Velazco et al., J.Chem.Phys. 65 (1976), 3468.
7. V.Boffa et al., SPIE 701, pg.158, ECOOSA '86.
8. G.C.Tisone et al., IEEE J.Quantum Electron. QE-18 (1982), 1008.
9. J.H.Jacob et al., J.Appl.Phys. 50 (1979), 5130.
10. M.Hunter et al., IEEE J.Quantum Electron. QE-22 (1986), 386.
11. C.P.Christensen et al., Opt.Lett. 12 (1987),169.
12. L.G.Wiley et al., Appl.Phys.Lett. 35 (1979), 239.
13. M.S.Arteev et al., Sov.J.Quantum Electron. 16 (1986), 1448.
14. M.A.Prelas et al., Laser & Particle Beams 6 (1988), 25.
15. W.H.Long Jr.and M.L.Bhaumik, J.de Physique 40 (1979),C7,127.
16. J.I.Levatter, S.C.Lin, J.Appl.Phys. 51 (1980), 210.
17. K.Midorikawa et al., IEEE J.Quantum Electron. QE-20 (1984), 198.
18. G.Stielow et al., Appl.Phys.B 47 (1988), 333; M.Ohwa, M.Obara, J.Appl.Phys. 59 (1986), 32;
    M.Maeda et al., Jap.J.Appl.Phys. 21 (1982), 1161; H.Hokazono et al., J.Appl.Phys. 56 (1984), 680.
19. a) M.R.Osborne, M.H.R.Hutchinson, J.Appl.Phys. 59 (1986),711;
    b) R.S.Taylor, Appl.Phys.B 41 (1986),1.
20. J.Coutts,C.E.Webbs, J.Appl.Phys. 59 (1986),704.
21. T.Hermsen, Opt.Comm. 64 (1987), 59.
22. C.A.Luca and H.N.Rutt, Opt.& Laser Techn. 21 (1989),99.
23. T.Letardi et al., ENEA Technical Report, RT/TIB/87/49.
24. a) W.W.Rigrod, IEEE J.Quantum Electron., QE-14 (1978), 377;
    b) G.M.Schindler, IEEE J.Quantum Electron. QE-16 (1980), 546;
    c) D.Eimerl, J.Appl.Phys. 51 (1980),3008.
25. T .Hermsen, to be published on ENEA Technical Report.
26. A.E.Siegman, Appl.Opt. 13 (1974), 353.
27. a) P.G.Gobbi, G.C.Reali, Opt.Comm. 52 (1984), 195;
    b) V.Boffa et al., IEEE J.Quantum Electron. QE-23 (1987), 1241.
28. P.Di Lazzaro et al., Appl.Phys.B 39 (1986),131;
    D.T.J. McKee and G.T. Boyd, Appl. Opt. 27 (1988), 1810.
29. a) J.P.Partanen, M.J.Shaw, Appl.Phys.B 43 (1987),231;
    b) T.J.Pacala et al., Appl.Phys.Lett. 45 (1984), 507.
30. a) Efthimiopoulos et al., Can.J.Phys. 57 (1979), 1437;
    b) C.P.Christensen et al., Appl.Phys.Lett. 29 (1976), 424.
31. G.Reksten et al., Appl.Phys.Lett. 39 (1981), 129.
32. a) J.H.Glownia et al., J.Opt.Soc.Am.B 4 (1987), 1061;
    b) S.Szatmari et al., Opt.Comm. 63 (1987), 305;
    c) S.Watanabe, Opt.Lett. 13 (1988), 580.
33. R.L.Fork et al., Opt.Lett. 9 (1984), 150.
34. R.S.Taylor and K.L.Leopold, J.Appl.Phys. 65 (1989), 22.
35. W.G.Long et al., Appl.Phys.Lett. 62 (1987), 735.
36. L.F.Champagne et al., J.Appl.Phys. 62 (1987), 1576.
37. Lasers & Optronics, January 1989, pg.8.
38. Laser Focus, September 1988, pg.8.

39. J.K.Rice et al., IEEE J.Quantum Electron. QE-16 (1980), 1315.
40. A.De Angelis et al., Appl.Phys.B 47 (1988), 1.
41. G.Giordano et al., ENEA Technical Report RT/TIB/87/65.